Modeling of low-energy charged particles passage through GAMMA-400 gamma-telescope thermal insulation and two-layer plastic scintillation detectors used as anticoincidence shield

E N Chasovikov, I V Arkhangelskaja, A I Arkhangelskiy, M D Kheymits, Yu T Yurkin
National Research Nuclear University MEPhI (Moscow Engineering Physics Institute), Kashirskoe highway 31, Moscow 115409, Russia

E-mail: e.chasovikov@gmail.com

Abstract. The results of low-energy charged particles passage through GAMMA-400 gamma-telescope thermal insulation and two-layer plastic scintillation detectors used as anticoincidence shield are presented. An existing GEANT4 GAMMA-400 model is used. Effects of thermal insulation on charged particle passage are investigated. These results will be used to testing the effect of low-energy charged particles flux on GAMMA-400 gamma-quanta registration capabilities. Sufficiently large energy deposition in two-layer plastic anti-coincidence scintillation detectors might interfere with high-energy particle registration and identification. However, GAMMA-400 detection capabilities are not affected by this, as the energy deposition in the lower layer of S3 is less than 1.5 MeV in all simulated cases. This value is less than threshold for high energy particles identification start (2.5 MeV). It makes impossible to incorrectly identify a low-energy charged particle energy deposition as backsplash from a high-energy gamma-quantum.

1. Introduction

GAMMA-400 is a space gamma-ray telescope project currently being developed by the international collaboration of the same name. It's main scientific objectives include study of high energy cosmic rays, galactic and extragalactic gamma-ray sources, gamma-ray bursts and dark matter [1-4]. This gamma-ray telescope will be covered by thermal insulation to provide thermal balance.

In order to determine quantitative properties of interactions of elementary particles with detector material and structural materials of the spacecraft a mathematical model is required.

GAMMA-400 orbit is located both within and outside magnetosphere. During its lifetime, GAMMA-400 will be exposed to low-energy charged particle flux [5], which may detrimentally affect it's anticoincidence system.

The main objective of this paper is to model the interaction between low-energy charged particles and thermal insulation and energy deposition in gamma-ray telescope detection systems.

2. Implementation

An existing Geant4 environment computer model of GAMMA-400 with all engineering elements included was used [6].

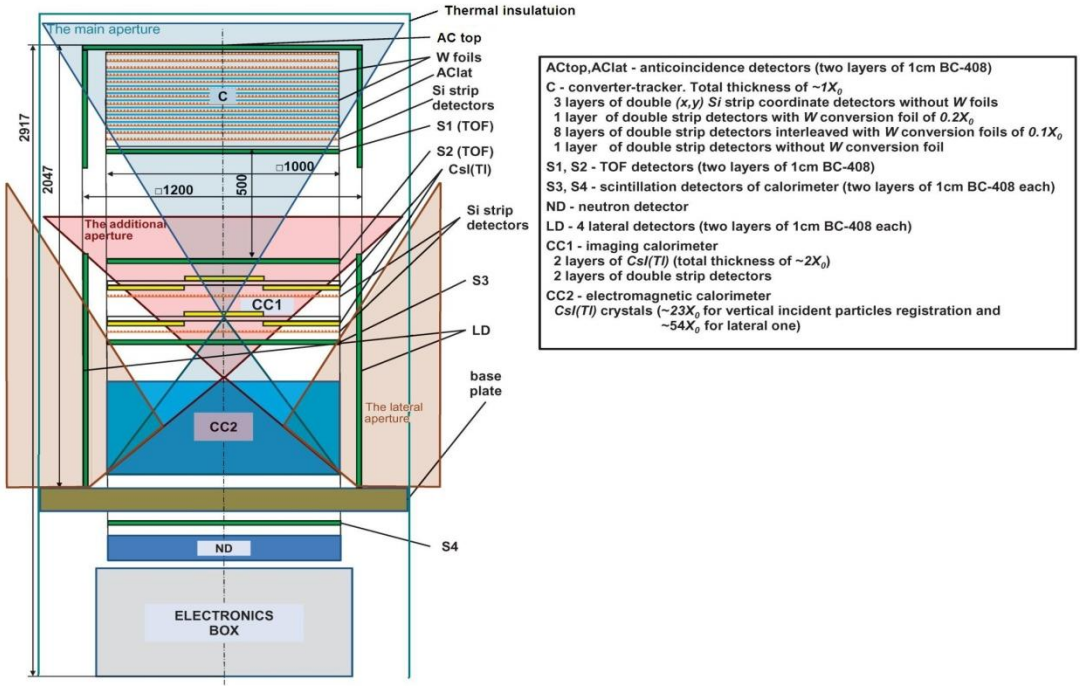

Figure 1. Principal scheme of GAMMA-400 with thermal insulation included

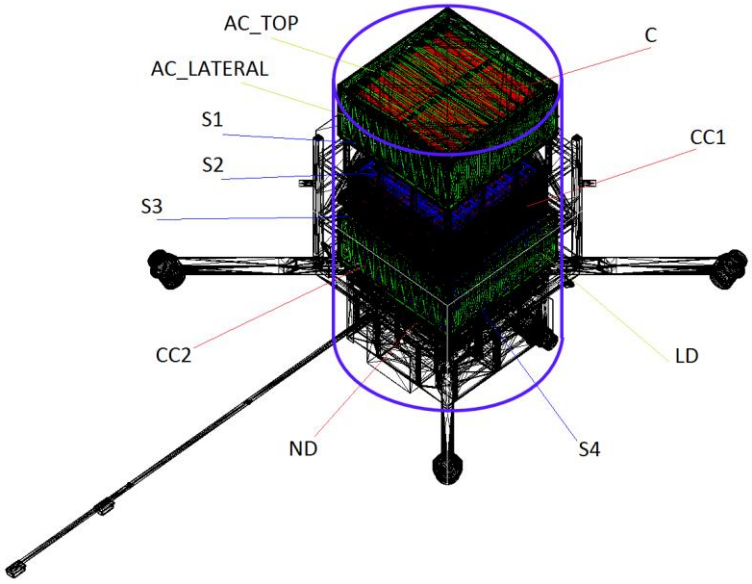

Figure 2. Layout of gamma-telescope GAMMA-400 in Geant4 environment

The principal scheme of GAMMA-400 is shown figure 1. This gamma-telescope consists of the following systems:

- Anticoincidence system top section ACtop
- Anticoincidence system lateral section AClat
- Calorimeter lateral anticoincidence LD System
- Time of flight system detector S1
- Time of flight system detector S2

- Position-sensitive calorimeter CC1
- Electromagnetic calorimeter CC2
- Scintillation detectors of calorimeter S3 and S4
- Neutron detector

All plastic detection systems (AC top, AC lat, LD, S1, S2, S3, S4) are composed of two layers of individual detectors [7].

In the main aperture triggers will be formed using information about particle direction provided by TOF system due special TOF signals matrix analyzed in the system of counting and triggers signals formation [8] for high-energy particles and presence of charged particle or backsplash due analysis of energy deposition in ACtop, S1, S2, S3.

The thermal insulation is modeled as a cylinder consisting of 1 layer of polyamide-6 ([-NH-(CH2)5-CO-]n), density 1.1g/cm^3, thickness 0.7mm and 2 aluminum foil layers, thickness 0.01mm each. Gamma-telescope GAMMA-400 layout in Geant4 environment is shown in figure 2 [6].

Passage of the following particle sets was simulated for the main aperture of gamma-telescope:

1. 10000 of 1 MeV electrons
2. 10000 of 3 MeV electrons
3. 10000 of 10 MeV electrons
4. 10000 of 30 MeV protons
5. 10000 of 100 MeV protons.

Sets 1 and 2 are selected to observe the difference between behavior of electrons interacting with matter only by Compton scattering and electrons being able to create photons due to bremsstrahlung. Set 3 represents the upper limit of trapped electron energy [9]. Set 4 is used to simulate low-energy protons expected to be absorbed by AC top upper layer [10]. Set 5 represents a proton capable of forming time-of-flight system signal [8].

Table 1. Amount of particles with non-zero energy deposition in plastic detectors.

Detector layer	e- 1MeV	e- 3MeV	e- 10MeV	Proton 30 MeV	Proton 100 MeV
AC top upper level	161	9834	9992	9936	9996
AC top lower layer	75	401	9640	38	9936
S1 upper layer	0	17	122	2	256
S1 lower layer	1	16	123	0	225
S2 upper layer	0	4	77	5	100
S2 lower layer	0	11	75	3	85
S3 upper layer	0	4	16	0	7
S3 lower layer	0	1	12	0	3

Table 2. Maximal energy deposition in plastic detectors, MeV.

Detector layer	e- 1MeV	e- 3MeV	e- 10MeV	Proton 30 MeV	Proton 100 MeV
AC top upper level	0.199	2.668	9.343	20.983	96.570
AC top lower layer	0.261	1.659	6.069	5.823	79.943
S1 upper layer	0	0.766	3.371	1.364	17.906
S1 lower layer	0.450[a]	0.875	3.948	0	21.944
S2 upper layer	0	0.322	2.831	0.467	13.779
S2 lower layer	0	0.320	1.926	0.975	2.468
S3 upper layer	0	0.255	0.904	0	1.225
S3 lower layer	0	0.041[a]	0.705	0	0.021

[a] These values are based only on single incidence, and should be interpreted as mean values of Landau distribution

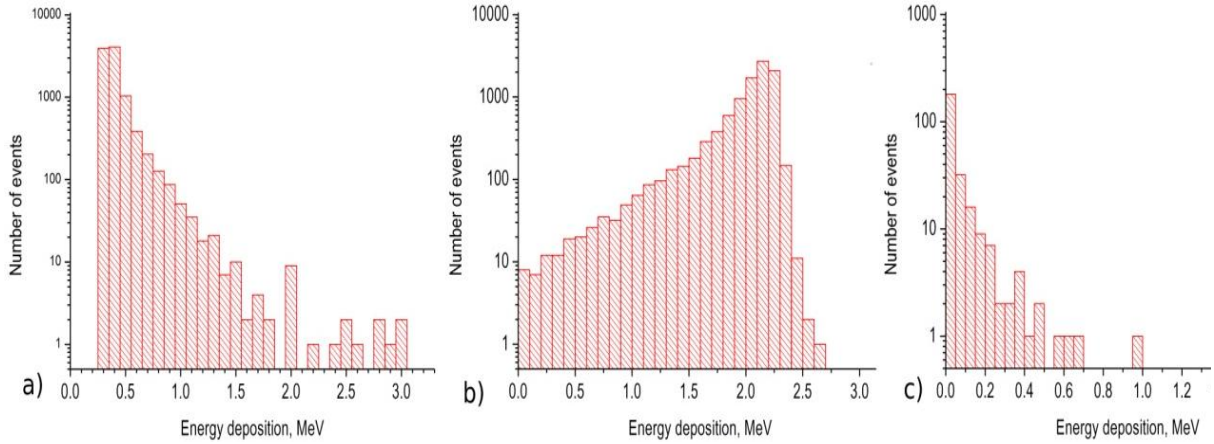

Figure 3. Energy deposition of 3 MeV electrons in a) thermal insulation b) upper layer of AC top c) lower layer of AC top.

As example, the energy deposition of 3 MeV electrons is represented in figure 3. The histograms in figure 3 take into account only particles interacting with a given layer.

The precise amount of particles with non-zero energy deposition is listed in table 1. Table 2 contains the maximal values of energy deposition in plastic detectors. As shown in table 1, the majority of electrons with energy of up to 3 MeV and protons with energy of up to 30 MeV didn't reach the lower layer of AC top, and 97% of all simulated particles were absorbed before entering S1. According to the data in table 2, the energy deposition in the lower layer of S3 is less than 1.5 MeV in all simulated cases, which makes it impossible to incorrectly identify a low-energy charged particle energy deposition as backsplash from a high-energy γ-quantum [8].

Based on data from GEOTAIL [11, 12] and Ulysses experiments [13, 14], known charged particle energy spectra [15, 16] and area of GAMMA-400 individual plastic detectors, the expected particles fluxes will be ~1.3×10^3 s^{-1} (for electrons with E>1 MeV) and ~10 s^{-1} (for protons with energy at least 30 MeV). This is not enough to cause significant dead time in GAMMA-400 detector systems because of energy deposition in S3 is less than threshold for high energy particles identification start (2.5 MeV [8]) – see tables 1, 2.

3. Conclusion

Passage of low-energy charged particles through GAMMA-400 gamma-telescope thermal insulation and two-layer plastic scintillation detectors used as anticoincidence shield was modeled.

The majority of electrons with energy of up to 3 MeV and protons with energy of up to 30MeV were absorbed before entering the lower layer of AC top.

The energy deposition in the lower layer of S3 is less than 1.5 MeV in all simulated cases. This value is less than threshold for high energy particles identification start (2.5 MeV [8]). It makes impossible to incorrectly identify a low-energy charged particle energy deposition as backsplash from a high-energy gamma-quantum.

Acknowledgments

This work performed within the framework of the Center FRPP supported by MEPhI Academic Excellence Project (contract No. 02.a03.21.0005, 27.08.2013).

References

[1] Topchiev N P *et al*. 2015 *Bull. Russ. Acad. Sci. Phys*. **79(3)** 417
[2] Topchiev N P *et al*. 2015 arXiv:1507.06246

[3] Galper A M *et al*. 2013 *Bull. Russ. Acad. Sci. Phys.* **77(11)** 1339
[4] Galper A M *et al*. 2013 *Advances in Space Research.* **51** 297
[5] Khyzhniak E V *et al*. 2015 *Phys. Proc.* **74** 238
[6] Chasovikov E N *et al*. 2015 *Phys. Proc.* **74** 206
[7] Runtso M F *et al*. 2015 *Phys. Proc.* **74** 220
[8] Arkhangelskaja I V *et al*. 2015 *Phys. Proc.* **74** 212
[9] Baker D N *et al.* 1986 *AGARD, The Aerospace Environment at High Altitudes and its Implications for Spacecraft Charging and Communications* **4-1** 406
[10] Sternheimer R M *et al* 1982 *Phys. Rev. B* **26(11)** 6067
[11] URL: http://pwg.gsfc.nasa.gov/geotail.shtml
[12] URL: http://cdaweb.gsfc.nasa.gov/istp_public/.
[13] URL: http://solarsystem.nasa.gov/missions/profile.cfm?MCode=Ulysses
[14] URL: http://ulysses.jpl.nasa.gov/science/data.html
[15] Hayakawa S 1969, *Cosmic Ray Physics* (New York , Wiley-Interscience)
[16] Olive K A *et al* 2014 Chin. Phys. C **38** 090001